Development of new composite fibers with excellent UV radiation protection

Nabil Bouazizi, Ahmed Abed, Stéphane Giraud, Ahmida El Achari, Christine Campagne, Mohammad Neaz Morshed, Olivier Thoumire, Reddad El Moznine, Omar Cherkaoui, Julien Vieillard, et al.

HAL Id: hal-02538228

https://normandie-univ.hal.science/hal-02538228

Submitted on 21 Jul 2022

Development of New Composite Fibers with Excellent UV Radiation Protection

Nabil Bouazizi [a,b*], Ahmed Abed [a, c, d], Stéphane Giraud [a], Ahmida El Achari [a], Christine Campagne [a], Mohammad Neaz Morshed [a], Olivier Thoumire[e], Reddad El Moznine [c], Omar Cherkaoui [c], Julien Vieillard[b] , Franc Le Derf[b]

[a] ENSAIT, GEMTEX – Laboratoire de Génie et Matériaux Textiles, F-59000 Lille, France
[b] Normandie Univ., UNIROUEN, INSA Rouen, CNRS, COBRA (UMR 6014), 55 rue Saint Germain, 27000 Evreux, France
[c]Laboratory LPMC, Faculty of Science El Jadida, Chouaib Doukkali University, El Jadida, Morocco.
[d]Laboratory REMTEX, ESITH, Route d'El Jadida, km 8, BP 7731 – Oulfa, Casablanca, Morocco
[e]Normandie Univ., UNIROUEN, CNRS, PBS (UMR 6270), 55 rue Saint Germain, 27000 Evreux, France

*CORRESPONDING AUTHORS.
Dr. Bouazizi Nabil: E-mail addresses bouazizi.nabil@hotmail.fr

GRAPHICAL ABSTRACT

Abstract

This work reports the design and functionalization of new composite-based polyester fibers with high anti UV radiation. Polyethylene terephthalate fibrous nonwovens were coated

1

by titanium dioxide, zinc oxide and silicon oxide. Chitosan and polyvinylidene fluoride polymers were used to ensure the good surface compatibility of the resulting composite PET-PVDF-OM-CT. These composites were fully characterized and the chemical coatings, surface modification, physical and thermal properties were investigated. Incorporation of metallic oxides resulted in the formation of strong cross-linked chitosan network. The developed modification on PET nonwovens allows to highly reducing the UV radiation with an excellent blocking rate and a good UV protection factor (80.5–113.4). An outline mechanism is proposed for the UV protection. This was explained by the surface compatibly and the interfacial bonding occurred in the matrix. Regarding to the above results, the current work developed a facile process for the production of advanced materials based nonwovens with excellent UV blocking.

Keywords: Polyester nonwovens; polyvinylidene fluoride; Chitosan; Metallic oxide; Thermal properties; UV Radiation;

1. Introduction

Nowadays, consumers are increasingly demanding multifunctional products. Textile sector have pied a quite intention to produce a clothes with great comfort and protection to the user since the clothes that related to environmental safety are necessary for consumers in their buying decision [1]. For these reasons, the great challenge for the textile industry is to fabricate durable and functional clothes using raw materials, low cost and ecofriendly [2-4]. Sunlight is necessary for human bodies in order to solicit the metabolism process, enhance blood operation and then increase the risk from many danger pathogens [5]. Herein, the harmful UV- radiation received from sun into skin for long time produces skin diseases, as premature ageing, allergies, sunburn and skin cancer [6]. For these reasons, using of anti-UV materials is of great importance to resolve the above problem issue from sunlight. On the other hand, despite the interesting properties of polyester nonwovens, some characteristics

like the inherently hydrophilic property, low mechanical resistance and insufficient sensitivity to the UV light, confine their wide applications, especially in some high-ends areas for medicine, catalysis, personal healthcare and self-cleaning [7-9]. Therefore, value addition to PET nonwovens by functionalization produced considerable industrial attention, attributed to their potential use in physical, thermal, biological and medical protection.

Textiles from synthetic fibers can present a highly negative impact on their hygiene and conservation properties. They supply the nutrients and proper growing environment for microorganisms, with suitable temperature, humidity, and oxygen. Therefore, the control and/or inhibition of microbiological growth are needed to protect both the user and the material itself [4, 10]. The ability of textiles to protect users against UV radiation depends on many factors, namely the chemical composition of the fibers, thickness, and mass per unit area.

Up to now, meterials oxides (MOx) [11] and their included hydroxyl groups showed that UV radiation can be refracted through decomposition reactions [12] and then induced an increase in the UV radiation protection [13].

On the other hand, the incorporation of MOx was used as elements for UV protection [14]. Meterials oxides have received considerable attention in several environmental applications, as it has many interesting properties that combined the mechanical, electrical, optical and biological properties [15]. Among them, zinc oxide (ZnO), titanium dioxide (TiO$_2$) [16, 17] and silicon dioxide (SiO$_2$) are widely studied in many aspects and were the most efficient candidates due to their important application in UV light-emitters, transparent electronics, varistors, surface acoustic wave devices, piezoelectric transducers and solar cells [18, 19]. The modification with organic substance makes great contribution to the dispersion of fillers and its strengthened barrier effect properties [20]. The introduction of transition metal

3

elements into polymer as a part of anti-UV radiation arouses great attention of researchers [21].

Intensive researches have been focused on developing advanced nanocomposites with improved surface properties by using these MOx. Yao et al. have found that adding Fe_3O_4 accelerates the carbonization of chlorinated poly(vinyl chloride) microfibers [22]. In this regard, MOx was activated and modified by the addition of some active agents such as amine derivate for enhancing electrical and sensing properties or polyvinylidene fluoride (PVDF) to increase the surface area and the adsorption properties [23]. Due to their excellent mechanical, chemical and eco-friendly properties, polyvinylidene fluoride was widely used various applications such as microfiltration and in advanced water separation and environmental remediation processes. Thus, nanocomposites based PVDF and MOx provided high thermal stability, mechanical properties, and impact resistance [24]. This was explained by the presence of PVDF which incorporates MOx, but also by the possible crosslink with the material [25]. In this aim, researchers have employed some natural polymers as chitosan which show many advantages over artificial materials [26, 27]. Recently, the chitosan was established as a good candidate in total biodegradability, biocompatibility with plants, antimicrobial, non-toxicity and fiber formation properties [28]. Thus, chitosan is one of the most prospective materials for many fields as wastewater treatment, pulp and paper, agriculture, and textile fields [29]. Indeed, in this contribution, polypropylene nonwoven-based composite separator was developed by modification through physical coating polymer and other elements, where the coating materials were helpful for the improvement of mechanical properties [30] when optimizing particle distribution and surface compatibility.

To the best of our knowledge, studies relating to a combination of all these additives have not been reported. On the basis of the above ideas, polyester nonwovens (PET) were employed for the fixation of materials oxides (MOx) like TiO_2, ZnO, and SiO_2, with the

presence of poly (vinylidene fluoride) (PVDF) as binder. Then, chitosan (CT) was employed as natural polymer to reinforce the immobilization of PVDF-MOx into nonwovens fibers. The obtained composites PET-PVDF-MOx-CT were used as sustainable materials to reduce UV radiation. Different modified nonwoven were systematically characterized by field emission scanning electron microscopy (SEM), optical microscopy, Fourier transforms infrared (FT-IR) spectroscopy, thermogravimetric analysis (TGA). The surface compatibility and the changes of UV radiation were investigated on the basis of the material structure and stability.

2. Experimental
2.1. Materials

Poly (vinylidene fluoride) 99% (PVDF), inorganic nanoparticles ZnO and TiO_2 were purchased from Sigma-Aldrich. SiO_2 nanoparticles were synthesized by sol-gel synthesis and the protocol is described in supporting file. Acetone and N, N-dimethylformamide 98.9% (DMF), ethanol, sodium triphosphate (PPT), distilled water, ammonia hydroxide 99% (NH_4OH, NH_3 basis), sodium hydroxide (NaOH) and tetraethoxysilane 97.98% (TEOS) were obtained and used as obtained. Polyester nonwovens (PET) with 0.9µm fiber diameter were obtained from CETI (**supporting information**).

2.2. Preparation and design of composite separator

Scheme. 1 illustrates the preparation and design route employed for separator construction and synthesis. The process mainly consisted of the following steps:

a. Firstly, in order to remove impurities and spinning oil present on the surface, the polyester (PET) nonwoven was treated according to our previously published work [31, 32]. Briefly, PET was activated by air atmospheric plasma to introduce both –OH and –COOH groups at the fiber surface (**supporting information**)[33].

b. Secondly, three solutions were prepared, containing differents metallic oxide (5%) (i.e. TiO_2, ZnO or SiO_2) and (7%) PVDF as reagents with a weight ratio (3:5) and a mixture of acetone and DMF (45:5 v/v) as solvent. The resulting solution was stirred for 2 h at 50 °C. After that, PET nonwovens were impregnated into the dispersed solution for 2 hours. The coated nonwovens were taken out from the solution and dried in at 50 °C for 24 h to clean and remove residual solvent in the resulting PET-PVDF-TiO_2, PET-PVDF-SiO_2, and PET-PVDF-ZnO composites.

c. Thirdly, each composite (i.e. PET-PVDF-MOx) was prone to the chemical grafting of chitosan (3%) CT by padding with an aqueous solution of 3 g/L chitosan polymer in presence of sodium triphosphate (PPT). The fabric was then dried (110 °C, 3 min) and cured (170 °C, 30 s) using a hot air dryer (Werner Mathis AG, Switzerland).

d. Finally, the obtained products denoted PET-PVDF-MOx-CT was hot-pressed before further characterization and tests.
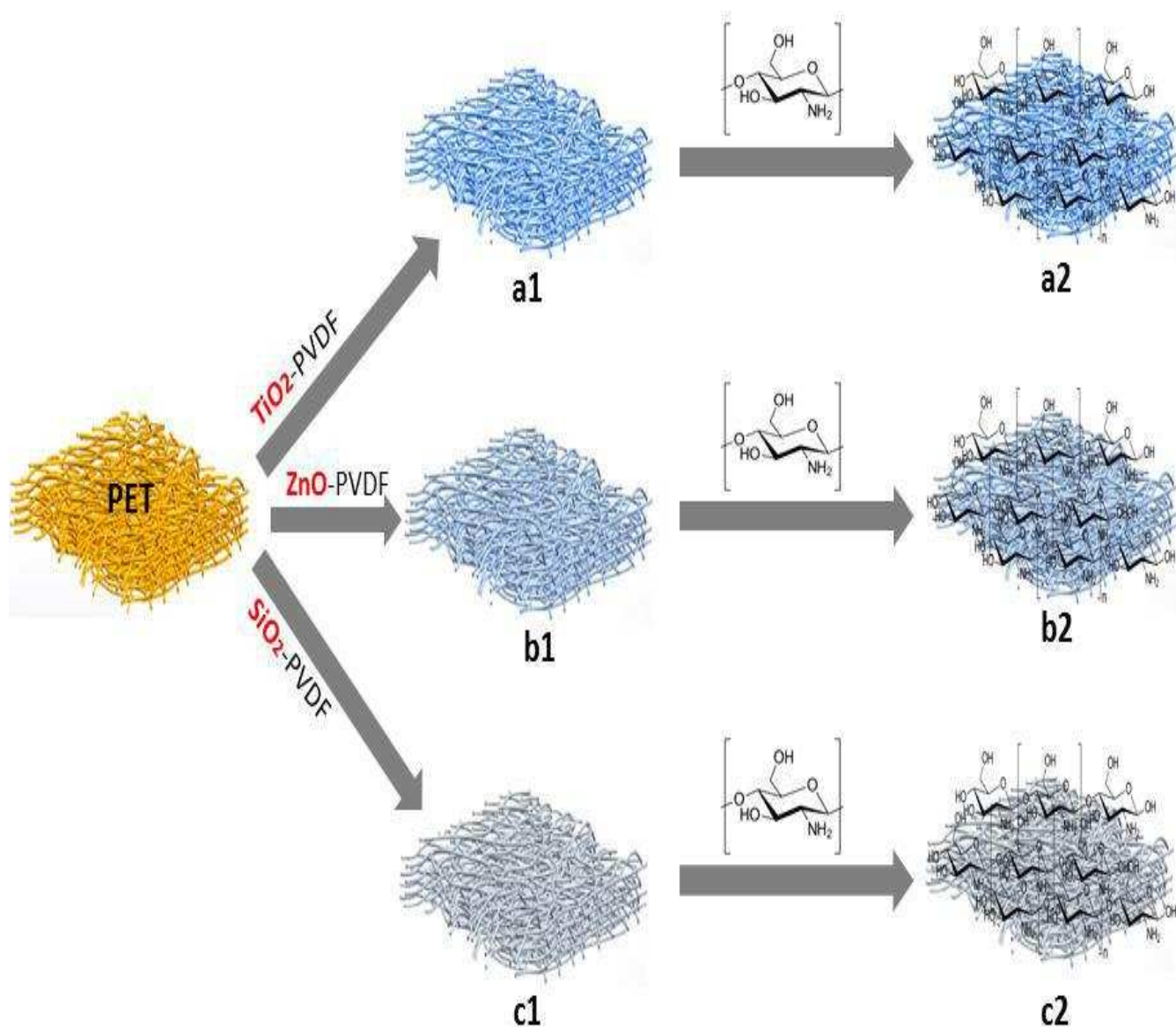
Scheme.1: Schematic illustration of the synthetic procedure of (a1) PET-PVDF-TiO$_2$, (a2) PET-PVDF-TiO$_2$-CT, (b1) PET-PVDF-ZnO, (b2) PET-PVDF-ZnO-CT, (c1) PET-PVDF-SiO$_2$ and (c2) PET-PVDF-SiO$_2$-CT materials.

2.3. Characterizations

The treated and original PET nonwovens were fully characterized in this work. Fourier transform IR spectroscopy was carried out using a Tensor 27 (Bruker) spectrometer with a ZnSe ATR crystal. The samples were analyzed by FTIR directly without any further preparation, and background spectra were recorded on air. For field emission scanning

electron microscopy (SEM) using a JEOL JEM-ARM200F HR setting with a field emission gun and probe aberration corrector, materials were previously metalized by a gold layer at 18 mA for 360 s with a Biorad E5200 device, and EDX images to evaluate the chemical contrast. Thermal analysis was measured by thermogravimetric analysis (TG-DTA, A6300R). In each sample, three measurements were made. The structures of the samples were investigated by X-ray diffraction (XRD) on a Rigaku XRD diffractometer using CuKα radiation (1.54059 Å).

2.4. Ultraviolet radiation blocking

The UV-radiation transmission spectra (T %) of all prepared composites were investigated using Shimadzu UV 1650 PC spectrophotometer in the range of 280–400 nm. From the transmittance measurements, UV protection factor (UPF), blocking in UV-A (315–400) region (UVA) and blocking in UV-B (280–315) region (UVB) were calculated from instrument using AATCC Test Method 183-2010 and according to Australian/New Zealand standard and British standard (**Table. S1**) [34]. In order to ensure good analysis, each sample was evaluated two times at different measurement areas and the average was considered.

The measurements of Ultraviolet Protection Factor (UPF) UV-A/UV-B were deduced from the following equations:

$$\text{UPF} = \frac{\sum_{280nm}^{400nm} E_\lambda \; X \; S_\lambda \; X \; \Delta\lambda}{\sum_{280nm}^{400nm} E_\lambda \; X \; S_\lambda \; X \; T_\lambda \; X \; \Delta\lambda} \tag{1}$$

$$\text{T(UV-A)} = \frac{\sum_{315nm}^{400nm} T_\lambda \; X \; \Delta\lambda}{\sum_{315nm}^{400nm} \Delta\lambda} \tag{2}$$

$$T\text{(UV-B)} = \frac{\sum\limits_{280nm}^{315nm} T_\lambda \ X \ \Delta\lambda}{\sum\limits_{280nm}^{315nm} \Delta\lambda} \qquad\qquad \textbf{(3)}$$

$$\text{UV-A} = 100 - T(UV-A) \qquad\qquad \textbf{(4)}$$

$$\text{UV-B} = 100 - T(UV-B) \qquad\qquad \textbf{(5)}$$

Where UPF is the ultraviolet protection factor registered by the composite, E_λ is relative erythemal spectral effectiveness, S_λ is solar spectral irradiance, T_λ is average spectral transmittance of the fabrics (measured) and Δ_λ is the interval of measured wavelength (5 nm in the current work). The magnitudes $E\lambda$ and S_λ were obtained from the AATCC test method 183-2004. T(UV-A) and T(UV-B) are the percents of transmittance in the A- and B-ranges of ultraviolet, respectively. UV-A and UV-B are the ultraviolet protection factor in the A- and B-ranges of ultraviolet, respectively.

3. Results and Discussions

3.1. Impact of CT and PVDF

Scheme 2 shows example mechanisms taking place during the preparation and modification process of the PET nonwovens. Recently many researches developed composites based nonwovens for environmental application, by the action of functionalized fiber with both inorganic and organic elements. Such protocols make it possible to fabricate the novel type of composites based nonwovens that bind inorganic particles as MOx and organic moieties as polymers. The immobilization of MOx by chemical grafting and/or substitution by organic molecules remains a major challenge due to their high tendency to aggregate. Entrapment of MOx within PET fiber by organic macromolecules may favor stabilization

9

through a combination of electrostatic and steric factors [35]. Until now, a wide variety of inorganic supports has been tested for both chemical and physical properties.

In this regard, our motivation was to tailor surface properties in order to produce a uniform composite. Firstly, sufficient hydroxyl and carboxylic groups were created via plasma treatment, which facilitated the binding and the chemical grafting of surface-tailored PET fibers. Herein, we voluntarily focused on PVDF as solid candidate for MOx crosslinking into PET fiber. Hence, the elasticity of most macromolecules prevents good fixation of MOx and decreases the aggregation. Then, MOx could be further covered by another polymers film, as chitosan, to generate a fiber with two layers i.e. PVDF-MOx and CT (**Scheme 3**). This strategy introduces new functionalities to the fibers offering two benefits: *(i)* reinforced the MOx immobilization; *(ii)* limited the diffusion of holes from the MOx to the surface (will be discussed in 3.8 section), which enhances hydrophobic properties by suppressing the holes with the trapped electrons, as reported previouslt [35]. In addition these suggestion were confirmed by the SEM and FTIR analysis.
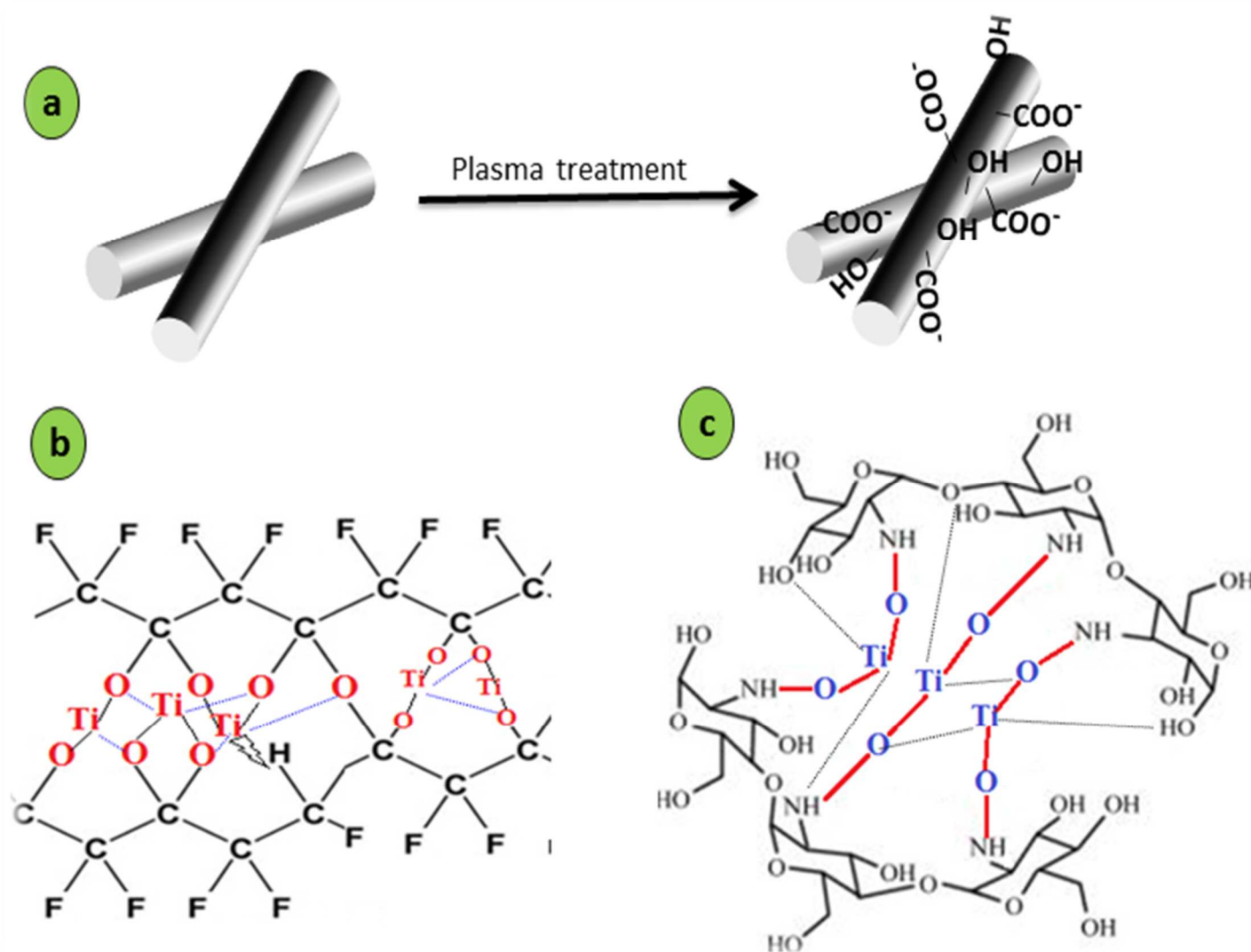
Scheme.2: Schematic illustration of (a) nonwovens fiber hydroxylation before, (b) PVDF-TiO$_2$ crosslinking and (c) possible interaction between chitosan and TiO$_2$.

3.2. Morphological properties

The surface morphology of untreated and treated PET nonwoven was determined by SEM analysis, and the results are shown in **Fig. 1**. The original PET nonwoven (**Fig. 1a**) exhibits a random network of overlapped fibers and multiple connected pores with a fairly smooth surface. From the PVDF coating process, the microstructure presented a continuous film structure with a thickness layer about a few microns, forming (**Fig. 1-c**). Visible changes were observed after the fixation of PVDF/MOx, indicating that PET surface was totally covered by

the PVDF/MOx particles (**Fig. d-e**). Regarding the good dispersion of MOx onto PET fibers, it was supposed that strong interfacial interactions between PET, PVDF, and MOx are involved. By comparing the treated PET (i.e. PET-PVDF-ZnO, PET-PVDF-SiO$_2$, and PET-PVDF-TiO$_2$), SEM images of PET-PVDF-TiO$_2$ showed a uniform distribution with high particles density at the fiber surface, resulting in a much smoother surface structure and the formation of bulkier clusters of much smaller particles. This fact can be explained in terms of strong interaction between PET:PVDF-MO$_x$, particularly for PET-PVDF-TiO$_2$, which promotes structure morphology with tailored surface, as supported in **Fig. 1**. In addition, from SEM images the thikness of PVDF, MOx and CT can be estimated as 2µm, 5µm and 1µm, respectively.
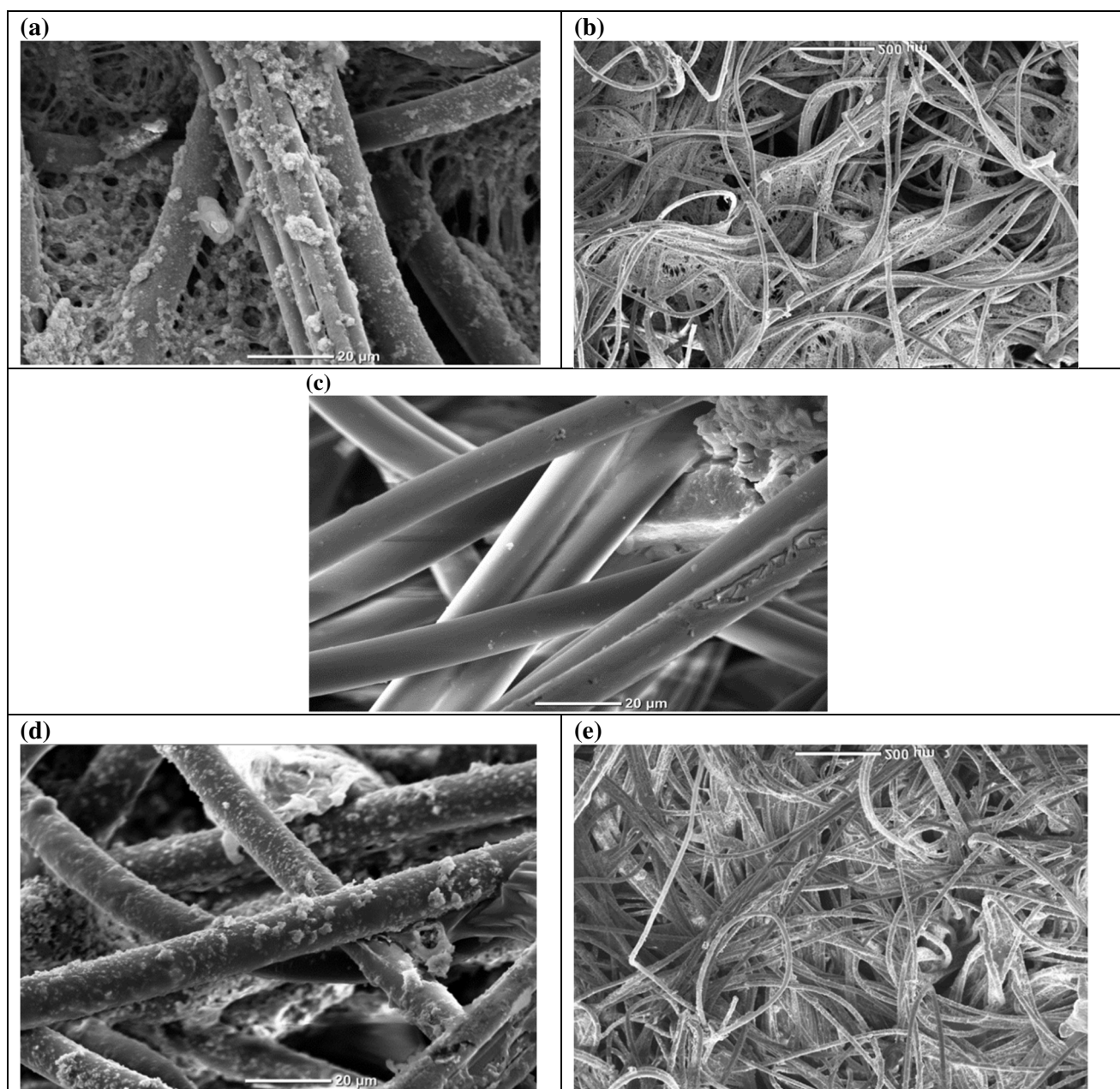
Figure.1: SEM images of (a) PET-PVDF-TiO$_2$-CT, (b) PET-PVDF-SiO$_2$-CT and (c) PET-PVDF-ZnO-CT materials.

3.3. XRD analysis

Figure S1 shows the XRD patterns of pure PET, PET-PVDF-SiO$_2$-CT, PET-PVDF-TiO$_2$-CT, and PET-PVDF-ZnO-CT composites. These patterns were recorded to analyze the

structure and crystalline phase of prepared MOx. The broad diffraction band observed 18° and

25° was attributed to the amorphous nature of the MOx. According to the JCPDS no 29-0085

and literature, the XRD diffraction of PET-PVDF-SiO$_2$-CT exhibits a broad peak centered at

$2\theta = 22°$. This peak is associated with the SiO$_2$ particles, which shows the successful addition

of amorphous SiO$_2$ in the PET fibers. For the PET-PVDF-TiO$_2$-CT pattern, the broader peaks

observed at 36.8° and 60.9° were due to the formation of TiO$_2$. Wile, the main peak observed

at $2\theta = 44°$ in the PET-PVDF-ZnO-CT pattern confirmed the presence of ZnO nanoparticles,

according to JCPDS card no 04 0850 [36]. In addition, XRD analysis confirms the successful

preparation of PET-PVDF-MOx-CT composites by EDX-XRF analysis, where elemental F,

N, Si, Ti, and Zn can be observed in the sample composition. The elemental F and N can be

observed in all spectrum of PET-PVDF-MOx-CT, suggesting the presence of PVDF and CT

in the materials. Elements of carbon and oxygen can also be observed in all EDX spectrums

which demonstrated the presence of various functional groups in the composites structure.

3.4. Infrared analysis

Infrared studies were carried out to ascertain the purity and nature of the functional

groups that exhibited on prepared composites. The FTIR spectra of original and modified PET

nonwovens are shown in (**Fig. 2**). The structure of original nonwoven displayed some bands

in the region 1720-650 cm^{-1}, attributed to the stretching vibration of CH$_2$, C=O, and aromatic

C=C. The peak observed at 3100 was attributed to the stretching vibration C-H present in the

polyester fibers. The broad absorption peaks at around 3437 and 1456 cm^{-1} are attributed to

stretching vibrations of OH groups corresponding to the adsorbed water molecules on the

sample's surface. After PVDF fixation, the bands obtained at 869 cm^{-1} were attributed to the

vibrations of υCF$_2$ for amorphous PVDF [37]. The chemical fixations of MOx were

confirmed by the presence of new supplementary peaks at low wavenumber. The band

observed at 515 cm^{-1} is attributed to the Zn–O stretching vibration, indicating the

characteristic band of pure ZnO [37]. The deposition of SiO_2 particles was confirmed by the enlargement of the band at 1100 cm^{-1} assigned to the stretching vibration of O−Si−O. Indeed, the impregnation of TiO_2 particles was confirmed by the band at 700 cm^{-1} assigned to the stretching vibration of Ti-O [38]. Chitosan grafting induced a shift of the υCF_2 peaks from 869 cm^{-1} to 875 cm^{-1} which might be due to the restriction on the vibration by the interaction occurred between TiO_2, CT and CF_2 groups [39]. The peak obtained at 1625 cm^{-1} was assigned to the NH_2 group bend scissoring, indicating that chitosan was successfully coated the modified PET fibers [40]. In addition, the band appeared at 1420 cm^{-1} and 1156 cm^{-1} were attributed to the OH bending of primary alcoholic group and to C-N stretch in chitosan, respectively. From the FTIR results, it can be summarized that CT, PVDF, and MOx are correctly attached to PET. We estimated that grafting occurs through the interaction of amine groups (–NH_2) and hydroxyl groups (–OH) through hydrogen bonding, which was in good agreement with hypothesis presented in the literature [41, 42].

Interestingly, the grafting of PVDF showed a characteristic peak appeared at 1108 cm^{-1} and assigned to the stretching vibration of the C-O-C band of PVDF. This peak was disappeared for both PET-PVDF-TiO_2 and PET-PVDF-TiO_2-PPT-CT modified nonwovens. This is due to the effective chemical grafting of PVDF, which involved specific interaction between C-F_2 in PVDF and TiO_2/CT. Deeper insights in the IR spectra of PET-PVDF-TiO_2 and PET-PVDF-TiO_2 -CT revealed a markedly decreases in the peaks intensity which provides significant evidence of the additional functional groups from the additives. The latter should confirm the good compatibility between PVDF and TiO_2-CT.
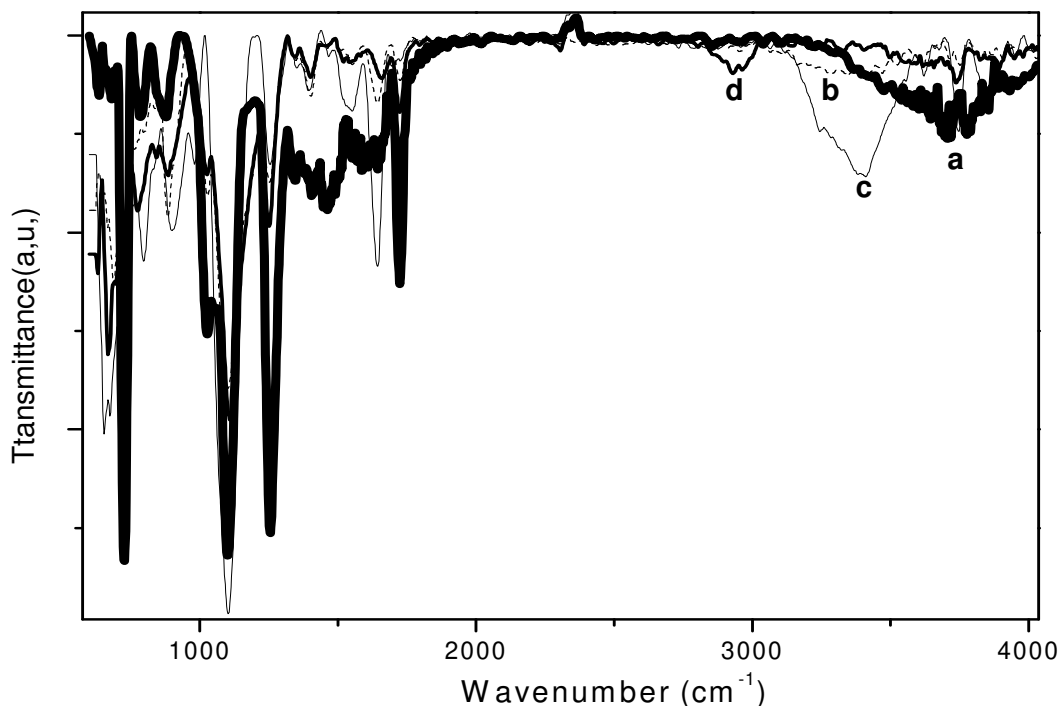
Figure. 2: FTIR spectra of (a) PET, (b) PET-PVDF-SiO$_2$-CT, (c) PET-PVDF-TiO$_2$-CT and

(d) PET-PVDF-ZnO-CT composites.

3.5. Thermogravimetric analysis

Thermogravimetric analysis was performed to provide onset temperature and analyze the thermal properties of the untreated PET and treated nonwovens composites. Under a nitrogen atmosphere, all samples were heated from room temperature to 800 °C at 20 °C/min and the results are shown in **figure. S3**. As first overview, the sample presents one single step for decomposition. The composite starts to decompose at 180–200 °C, which was in good agreement with previous reports [43, 44]. The primary mass loss at the range of 100-200 °C is assigned to the evaporation of adsorbed water and the later decomposition is ascribed to the depolymerization of both PVDF and CT as organic molecules. There is a mass increment process for PET-PVDF-MOx at the range of 300-400 °C, indicating the effect of MOx on the

16

thermal properties. Here, the initial decomposition temperature of PET, PET-PVDF-ZnO, PET-PVDF-TiO$_2$, and PET-PVDF-SiO$_2$ are 333°C, 335°C, 491°C and 480 °C, respectively. The high temperature at maximum weight loss rate can also be found for these hybrids, demonstrating again their good thermal stability, particularly for PET-PVDF-TiO$_2$ which confirm again the good dispersion of TiO$_2$ particles. The improvement on the PET-PVDF-TiO$_2$ is du to the good surface compatibility between all compouds (PET: PVDF; TiO$_2$; CT), especially for the TiO$_2$ particles. Alos, this changes can be explained in term of affinity and the suitable interaction between PVDF and TiO$_2$.

3.6. Tailoring interfacial compatibility in PVDF/MOx/CT

Scheme. 2 shows example mechanisms taking place during the preparation and modification process of the PET nonwovens. As the composites based nonwovens for environmental application, are prepared by the action of functionalized fiber with both inorganic and organic elements. The immobilization of MOx by chemical grafting and/or substitution by organic molecules remains a major challenge due to their high tendency to aggregate. Entrapment of MOx within PET fiber by organic macromolecules may favor stabilization through a combination of electrostatic and steric factors [45]. Until now, a wide variety of inorganic supports have been tested for both chemical and physical properties. In this regard, our motivation was to tailor surface properties in order to produce a uniform composite. Firstly, sufficient hydroxyl and carboxylic groups were created via plasma treatment, which facilitated the binding and the chemical grafting of surface-tailored PET fibers. Herein, we voluntarily focused on PVDF as solid candidate for MOx crosslinking into PET fiber. Hence, the elasticity of most macromolecules prevents good fixation of MOx and decreases the aggregation. Then, MOx could be further covered by another polymers film, as chitosan, to generate a fiber with two layers i.e. PVDF-MOx and CT. This strategy introduces new functionalities to the fibers offering two benefits: (i) reinforced the MOx immobilization; (ii)

17

limited the diffusion of holes from the MOx to the surface, which highly enhances hydrophobic properties by suppressing the holes with the trapped electrons (**Table.1**).

Table. 1: Evolution in time of the contact angle for PET and modified counterparts.

Samples	Contact angle (°)*
PET	20
PET-PVDF-TiO$_2$-CT	110
PET-PVDF-ZnO-CT	114
PET-PVDF-SiO$_2$-CT	108

* The measurements were carried out within 30 seconds at room temperature.

The compatibility of the composite chemicals was investigated and results are illustrated in the **scheme. 3**. It is indicated that is, the compatibility between hydroxyl groups on plasma modified polyester nonwovens and MOx is well established by the strong crosslinking. Besides, it was considered that the introduced polar groups could act as scattering centers or charge trapping sites in composites. The interface between MOx and CT, especially electrostatic distribution, provides fundamental information about the interfacial trap. Since the CT/MOx has a greater electrostatic force on the charge carriers nearby, the greater trapping effect is introduced in the interface sites in the prepared composite. Comprehensively, the different interaction energy could lead to the different interfacial compatibility between PVDF/MOx and the CT matrix and interfacial trapping effect on charge carriers. The interfacial compatibility and trap are closely related to the interaction energy and polyester nonwovens between functionalized groups on filler surface and polymer matrix. Likewise, according to the SEM pictures (**Fig. 1**), it shows that the interface between PVDF/TiO$_2$ and PET fibers matrix is more pronounced than that between those with ZnO and SiO$_2$ matrix.
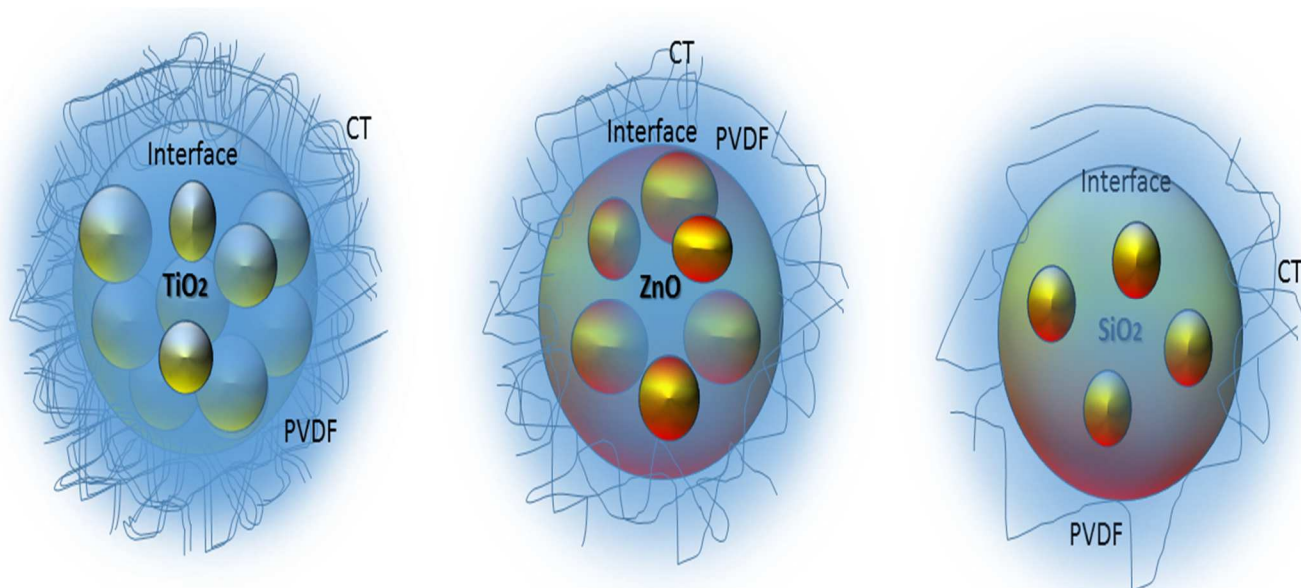
Scheme.3. Schematic illustration of different interfacial structure induced by PVDF/MOx/CT

3.7. Composites with high anti-UV radiation

The resistances against ultraviolet radiation (UVR) of functionalized composites were studied by the transmission in the region of 280 to 400 nm as UVR and the obtained results were reported in **Figure. 3**. As seen, all functional composites nonwovens demonstrated good UVR blocking properties. It is evident that the treatments with PVDF/MOx/CT considerably reduced the UV transmission through the sample. Particularly, PET-PVDF-TiO$_2$-CT displayed higher UVR blocking than the other counterparts. Thus, it was found that the functionalization steps were accompanied by high resistance to transmission in UVR near-zero T% = 1.6 (**Table 2**). Consequently, we are able to develop original nonwovens sample fully resistant to UVR. In this regard, confirmation was obtained by the measurements of transmission UVA and UVB in and regions, respectively. The blocking in UVA (315-400 nm) and UVB (280-315 nm) regions and ultraviolet protection factor (UPF) were calculated using AATCC test method and the results are summarized in **Table. 2**. As result, the transmission in UVA /UVB was (55.09/13.75); (40.40/4.36); (1.60/0.93) and (4.88/1.10) for PET, PET-

PVDF-SiO$_2$-CT, PET-PVDF-TiO$_2$-CT, and PET-PVDF-ZnO-CT, respectively (**Figure. S4**). Treatments with PVDF-TiO$_2$-CT showed high reduction in UVA and UVB until 0% in UVB. In addition, results on PET-PVDF-TiO$_2$-CT provided a dramatically widening of the UVA and UVB blocking (98.40% and 99.07%) in comparison to the untreated nonwovens (44.01% and 86.25%). Herein, the above results confirmed again the performance of the strategy that employed for surface functionalization, especially for sample that incorporated TiO$_2$.

According to the Australian/New Zealand standard and British standard, UPF was significantly increased from 49 for PET to 113.4 for PET-PVDF-TiO$_2$-CT. Afterward, PET-PVDF-SiO$_2$-CT composites with UPF values less than 10 are still considered as insufficient protective materials. However, for PET-PVDF-ZnO-CT, the UPF reached a value higher than 80 (80.50), which were judged as excellent UV protective composites. Interestingly, PET-PVDF-TiO$_2$-CT is considered as an excellent UV protective composite with UPF values 113.4. Here, PET-PVDF-TiO$_2$-CT showed much better UV protection properties, which was assigned to the significant higher titanium content in fiber surface. To the best of our knowledge, the functional PET-PVDF-TiO$_2$-CT composite appears to exhibit the highest UVR blocking property properties and UPF values as compared to other materials published elsewhere [44, 46-53].
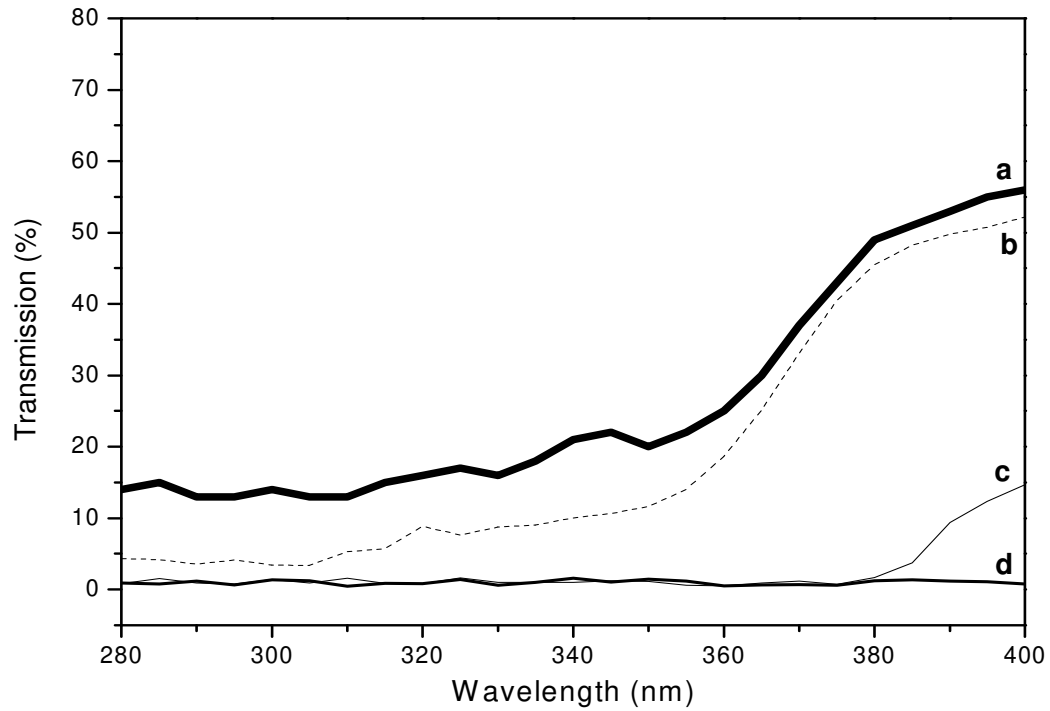
Figure. 3: Transmission of ultraviolet radiation for (a) PET, (b) PET-PVDF-SiO2-CT, (c)

PET-PVDF-ZnO-CT and (d) PET-PVDF-TiO$_2$-CT.

Table. 2: UV blocking results (according to AATCC test method) for PET, PET-PVDF-SiO$_2$-CT, PET-PVDF-ZnO-CT, and PET-PVDF-TiO$_2$-CT.

Samples	UVA (T%)	UVB (T%)	Blocking UVA	Blocking UVB	UPF	UPF rate
PET	55.09	13.75	44.01	86.25	6.49	Insufficient
PET-PVDF-SiO$_2$-CT	40.40	4.36	59.60	95.64	14.69	Insufficient
PET-PVDF-TiO$_2$-CT	1.60	0.93	98.40	99.07	113.40	Excellent
PET-PVDF-ZnO-CT	4.88	1.10	95.12	98.90	80.50	Excellent

3.8. Proposed mechanism

As expected, the higher efficiency of PET-PVDF-TiO$_2$-CT composite towards UV blocking properties may be attributed to three major relevant factors; *(i)* the good fixation of TiO$_2$ in presence of PVDF and CT allows covering construction and pores of nonwovens fibers and then blocks the interspaces. Consequently, the UV radiation can be reflected or diffracted easily and upon the contact with the composite interface (**Scheme 4**). Hence, *(ii)* the PVDF-TiO$_2$-CT contents onto fiber nonwovens had a higher density after using the thermal pressure resulted in efficient UVR blocking. Additionally, *(iii)* as PVDF, TiO$_2$ and CT reacted with nonwoven fibers, producing several stronger chemical bonds, which increase the solidity of the materials and improve again the UVR blocking. This was in agreement with the wash fastness results, as supported by the releases of particles during the washing process.
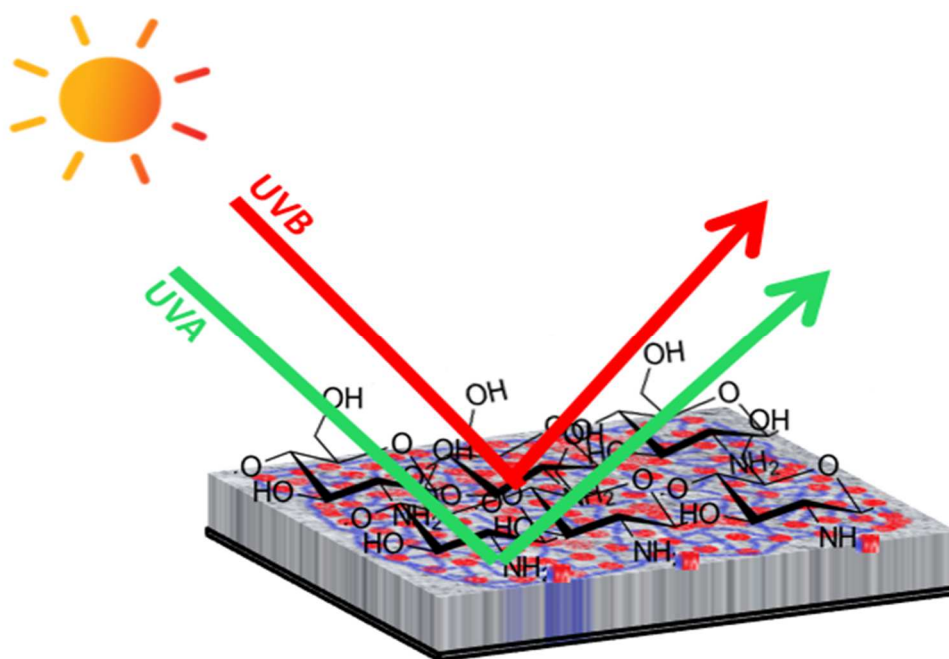
Scheme. 4: Reflection of UVA/UVB radiation on PET-PVDF-MOx-CT composites.

4. Conclusion

Regarding the high demand of the research in the field of UVR protection and durability of polymer composites, this work explored an overview of the design, application, and

mechanism of functional PET nonwoven for full blocking of UVR. It was found that fixation of PVDF/MOx/CT into PET fibers strongly enhanced both the UV protection and thermal stability of the composites materials. Interfacial compatibility has a significant role on the anti-UV protection of composites. Larger interaction energy reduces interfacial defects with a greater electrostatic force, demonstrating as the enhanced trapping effect. The developed treatment method can be used in textile industry to produce multifunctional nonwovens for safety and eco-environmentally applications. This new work can open many advanced ways for further research to activate natural and or synthetic textile and other objects for both human and environmental safety.

REFERENCES

[1] R. Paul, Functional finishes for textiles: an overview, Functional Finishes for Textiles, Improving Comfort, Performance and Protection, (2014) 1-14.

[2] N.A. Ibrahim, R. Refaie, A.F. Ahmed, Novel approach for attaining cotton fabric with multi-functional properties, Journal of Industrial Textiles, 40 (2010) 65-83.

[3] H. Yang, C.Q. Yang, Durable flame retardant finishing of the nylon/cotton blend fabric using a hydroxyl-functional organophosphorus oligomer, Polymer Degradation and Stability, 88 (2005) 363-370.

[4] M. Montazer, S. Seifollahzadeh, Enhanced self-cleaning, antibacterial and UV protection properties of nano TiO2 treated textile through enzymatic pretreatment, Photochemistry and photobiology, 87 (2011) 877-883.

[5] L. Hu, H. Zhang, A. Gao, A. Hou, Functional modification of cellulose fabrics with phthalocyanine derivatives and the UV light-induced antibacterial performance, Carbohydrate polymers, 201 (2018) 382-386.

[6] H. Qi, J. Pan, F.-l. Qing, K. Yan, G. Sun, Anti-wrinkle and UV protective performance of cotton fabrics finished with 5-(carbonyloxy succinic)-benzene-1, 2, 4-tricarboxylic acid, Carbohydrate polymers, 154 (2016) 313-319.

[7] H.E. Emam, R.M. Abdelhameed, Anti-UV radiation textiles designed by embracing with nano-MIL (Ti, In)–metal organic framework, ACS applied materials & interfaces, 9 (2017) 28034-28045.

[8] M.N. Morshed, N. Behary, N. Bouazizi, J. Guan, G. Chen, V. Nierstrasz, Surface modification of polyester fabric using plasma-dendrimer for robust immobilization of glucose oxidase enzyme, Scientific reports, 9 (2019) 1-16.

[9] B. Nabil, M.N. Morshed, B. Nemeshwaree, C. Christine, V. Julien, T. Olivier, A. Abdelkrim, Development of new multifunctional filter based nonwovens for organics pollutants reduction and detoxification: High catalytic and antibacterial activities, Chemical Engineering Journal, 356 (2019) 702-716.

[10] R. Dastjerdi, M. Montazer, A review on the application of inorganic nano-structured materials in the modification of textiles: focus on anti-microbial properties, Colloids and surfaces B: Biointerfaces, 79 (2010) 5-18.

[11] A. Gao, C. Zhang, K. Song, A. Hou, Preparation of multi-functional cellulose containing huge conjugated system and its UV-protective and antibacterial property, Carbohydrate polymers, 114 (2014) 392-398.

[12] R.S. Plentz, M. Miotto, E.E. Schneider, M.M.C. Forte, R.S. Mauler, S.M. Nachtigall, Effect of a macromolecular coupling agent on the properties of aluminum hydroxide/PP composites, Journal of applied polymer science, 101 (2006) 1799-1805.

[13] A.E. Shafei, A. Abou-Okeil, ZnO/carboxymethyl chitosan bionano-composite to impart antibacterial and UV protection for cotton fabric, Carbohydrate Polymers, 83 (2011) 920-925.

[14] N. Bouazizi, F. Ajala, A. Bettaibi, M. Khelil, A. Benghnia, R. Bargougui, S. Louhichi, L. Labiadh, R.B. Slama, B. Chaouachi, Metal-organo-zinc oxide materials: investigation on the structural, optical and electrical properties, Journal of Alloys and Compounds, 656 (2016) 146-153.

[15] N. Bouazizi, M. Khelil, F. Ajala, T. Boudharaa, A. Benghnia, H. Lachheb, R.B. Slama, B. Chaouachi, A. M'nif, A. Azzouz, Molybdenum-loaded 1, 5-diaminonaphthalene/ZnO materials with improved electrical properties and affinity towards hydrogen at ambient conditions, international journal of hydrogen energy, 41 (2016) 11232-11241.

[16] M.N. Morshed, X. Shen, H. Deb, S.A. Azad, X. Zhang, R. Li, Sonochemical fabrication of nanocryatalline titanium dioxide (TiO2) in cotton fiber for durable ultraviolet resistance, Journal of Natural Fibers, (2018) 1-14.

[17] M.N. Morshed, S. Al Azad, H. Deb, B.B. Shaun, X.L. Shen, Titania-loaded cellulose-based functional hybrid nanomaterial for photocatalytic degradation of toxic aromatic dye in water, Journal of Water Process Engineering, 33 (2020) 101062.

[18] D. Wang, L. Song, K. Zhou, X. Yu, Y. Hu, J. Wang, Anomalous nano-barrier effects of ultrathin molybdenum disulfide nanosheets for improving the flame retardance of polymer nanocomposites, Journal of Materials Chemistry A, 3 (2015) 14307-14317.

[19] H. Deb, M.N. Morshed, S. Xiao, S. Al Azad, Z. Cai, A. Ahmed, Design and development of TiO 2-Fe 0 nanoparticle-immobilized nanofibrous mat for photocatalytic degradation of hazardous water pollutants, Journal of Materials Science: Materials in Electronics, 30 (2019) 4842-4854.

[20] H. Deb, S. Xiao, M.N. Morshed, S. Al Azad, Immobilization of Cationic Titanium Dioxide (TiO 2+) on Electrospun Nanofibrous Mat: Synthesis, Characterization, and Potential Environmental Application, Fibers and Polymers, 19 (2018) 1715-1725.

[21] S.-D. Jiang, Z.-M. Bai, G. Tang, L. Song, A.A. Stec, T.R. Hull, Y. Hu, W.-Z. Hu, Synthesis of mesoporous silica@ Co–Al layered double hydroxide spheres: layer-by-layer method and their effects on the flame retardancy of epoxy resins, ACS applied materials & interfaces, 6 (2014) 14076-14086.

[22] K. Yao, J. Gong, J. Zheng, L. Wang, H. Tan, G. Zhang, Y. Lin, H. Na, X. Chen, X. Wen, Catalytic carbonization of chlorinated poly (vinyl chloride) microfibers into carbon microfibers with high performance in the photodegradation of Congo Red, The Journal of Physical Chemistry C, 117 (2013) 17016-17023.

[23] A. Ferrreira, J. Rocha, A. Ansón-Casaos, M. Martínez, F. Vaz, S. Lanceros-Mendez, Electromechanical performance of poly (vinylidene fluoride)/carbon nanotube composites for strain sensor applications, Sensors and Actuators A: Physical, 178 (2012) 10-16.

[24] H. Parangusan, D. Ponnamma, M.A.A. AlMaadeed, Flexible tri-layer piezoelectric nanogenerator based on PVDF-HFP/Ni-doped ZnO nanocomposites, RSC Advances, 7 (2017) 50156-50165.

[25] X. Guan, Y. Zhang, H. Li, J. Ou, PZT/PVDF composites doped with carbon nanotubes, Sensors and Actuators A: Physical, 194 (2013) 228-231.

[26] P. Huang, M. Cao, Q. Liu, Adsorption of chitosan on chalcopyrite and galena from aqueous suspensions, Colloids and Surfaces A: Physicochemical and Engineering Aspects, 409 (2012) 167-175.

[27] P. Huang, M. Cao, Q. Liu, Using chitosan as a selective depressant in the differential flotation of Cu–Pb sulfides, International Journal of Mineral Processing, 106 (2012) 8-15.

[28] J. Li, Y. Gong, N. Zhao, X. Zhang, Preparation of N-butyl chitosan and study of its physical and biological properties, Journal of applied polymer science, 98 (2005) 1016-1024.

[29] V.G. Dev, R. Neelakandan, S. Sudha, O. Shamugasundram, R. Nadaraj, Chitosan-a polymer with wider applications, TEXTILE MAGAZINE-MADRAS-, 46 (2005) 83.

[30] A.B. Shipovskaya, S.L. Shmakov, N.O. Gegel, Optical activity anisotropy of chitosan-based films, Carbohydrate polymers, 206 (2019) 476-486.

[31] V. Takke, N. Behary, A. Perwuelz, C. Campagne, Studies on the atmospheric air–plasma treatment of PET (polyethylene terephtalate) woven fabrics: effect of process parameters and of aging, Journal of applied polymer science, 114 (2009) 348-357.

[32] M.N. Morshed, N. Bouazizi, N. Behary, J. Vieillard, O. Thoumire, V. Nierstrasz, A. Azzouz, Iron-loaded amine/thiol functionalized polyester fibers with high catalytic activities: a comparative study, Dalton transactions (Cambridge, England: 2003), 48 (2019) 8384-8399.

[33] M.N. Morshed, N. Bouazizi, N. Behary, J. Guan, V. Nierstrasz, Stabilization of zero valent iron (Fe0) on plasma/dendrimer functionalized polyester fabrics for Fenton-like removal of hazardous water pollutants, Chemical Engineering Journal, 374 (2019) 658-673.

[34] A.T.M. 183-2004, Transmittance or Blocking of Erythemally Weighted Ultraviolet Radiation Through Fabrics, AATCC Technical Manual, 85 (2010) 318-321.

[35] Abed, Ahmed, et al. "Preparation of a novel composites based polyester nonwovens with high mechanical resistance and wash fastness properties." *Colloids and Surfaces A: Physicochemical and Engineering Aspects* 577(2019)604-612.

[36] S. Salar, M. Jafari, S.F. Kaboli, F. Mehrnejad, The role of intermolecular interactions on the encapsulation of human insulin into the chitosan and cholesterol-grafted chitosan polymers, Carbohydrate polymers, 208 (2019) 345-355.

[37] N. Bachan, A. Asha, W.J. Jeyarani, D.A. Kumar, J.M. Shyla, A Comparative Investigation on the Structural, Optical and Electrical Properties of SiO 2–Fe 3 O 4 Core–Shell Nanostructures with Their Single Components, Acta Metallurgica Sinica (English Letters), 28 (2015) 1317-1325.

[38] F. Ali, S.B. Khan, T. Kamal, K.A. Alamry, E.M. Bakhsh, A.M. Asiri, T.R. Sobahi, Synthesis and characterization of metal nanoparticles templated chitosan-SiO2 catalyst for the reduction of nitrophenols and dyes, Carbohydrate polymers, 192 (2018) 217-230.

[39] Z. Mai, Z. Xiong, X. Shu, X. Liu, H. Zhang, X. Yin, Y. Zhou, M. Liu, M. Zhang, W. Xu, Multifunctionalization of cotton fabrics with polyvinylsilsesquioxane/ZnO composite coatings, Carbohydrate polymers, 199 (2018) 516-525.

[40] A.K. Tripathi, M.K. Singh, M.C. Mathpal, S.K. Mishra, A. Agarwal, Study of structural transformation in TiO2 nanoparticles and its optical properties, Journal of Alloys and Compounds, 549 (2013) 114-120.

[41] Q. Zhou, X.-P. Lei, J.-H. Li, B.-F. Yan, Q.-Q. Zhang, Antifouling, adsorption and reversible flux properties of zwitterionic grafted PVDF membrane prepared via physisorbed free radical polymerization, Desalination, 337 (2014) 6-15.

[42] J. Coates, Encyclopedia of analytical chemistry, Interpretation of infrared spectra, a practical approach. Wiley, Chichester, (2000) 10815-10837.

[43] L.-y. Zhang, X.-j. Zhu, H.-w. Sun, G.-r. Chi, J.-x. Xu, Y.-l. Sun, Control synthesis of magnetic Fe3O4–chitosan nanoparticles under UV irradiation in aqueous system, Current Applied Physics, 10 (2010) 828-833.

[44] W. Ma, F.-Q. Ya, M. Han, R. Wang, Characteristics of equilibrium, kinetics studies for adsorption of fluoride on magnetic-chitosan particle, Journal of hazardous materials, 143 (2007) 296-302.

[45] N. Bouazizi, J. Vieillard, R. Bargougui, N. Couvrat, O. Thoumire, S. Morin, G. Ladam, N. Mofaddel, N. Brun, A. Azzouz, Entrapment and stabilization of iron nanoparticles within APTES modified graphene oxide sheets for catalytic activity improvement, Journal of Alloys and Compounds, 771 (2019) 1090-1102.

[46] Y. Feng, B. Miao, H. Gong, Y. Xie, X. Wei, Z. Zhang, High dielectric and mechanical properties achieved in cross-linked PVDF/α-SiC nanocomposites with elevated compatibility and induced polarization at the interface, ACS applied materials & interfaces, 8 (2016) 19054-19065.

[47] H.E. Emam, T. Bechtold, Cotton fabrics with UV blocking properties through metal salts deposition, Applied Surface Science, 357 (2015) 1878-1889.

[48] N. Vigneshwaran, S. Kumar, A. Kathe, P. Varadarajan, V. Prasad, Functional finishing of cotton fabrics using zinc oxide–soluble starch nanocomposites, Nanotechnology, 17 (2006) 5087.

[49] A. Becheri, M. Dürr, P.L. Nostro, P. Baglioni, Synthesis and characterization of zinc oxide nanoparticles: application to textiles as UV-absorbers, Journal of Nanoparticle Research, 10 (2008) 679-689.

[50] Z. Mao, Q. Shi, L. Zhang, H. Cao, The formation and UV-blocking property of needle-shaped ZnO nanorod on cotton fabric, Thin Solid Films, 517 (2009) 2681-2686.

[51] A. Sivakumar, R. Murugan, K. Sundaresan, S. Periyasamy, UV protection and self-cleaning finish for cotton fabric using metal oxide nanoparticles, (2013).

[52] H.B. Ahmed, H.E. Emam, Layer by layer assembly of nanosilver for high performance cotton fabrics, Fibers and Polymers, 17 (2016) 418-426.

[53] H.E. Emam, N. Saleh, K.S. Nagy, M. Zahran, Instantly AgNPs deposition through facile solventless technique for poly-functional cotton fabrics, International journal of biological macromolecules, 84 (2016) 308-318.